Available online at www.sciencedirect.com

ScienceDirect

Ceramics International 41 (2015) 11908–11917

CERAMICS INTERNATIONAL

www.elsevier.com/locate/ceramint

Analytical modeling of activation procedure applied in α-alumina thermo-mechanical synthesis

Anja Terzić[a,*], Lato Pezo[b], Ljubiša Andrić[c], Vojislav V. Mitić[d]

[a]Institute for Materials Testing, Vojvode Mišića Bl. 43, 11000 Belgrade, Serbia
[b]Institute of General and Physical Chemistry, University of Belgrade, Studentski Trg 12-16, 11000 Belgrade, Serbia
[c]Institute for Technology of Nuclear and other Raw Mineral Materials, Franchet d'Esperey 86, 11000 Belgrade, Serbia
[d]Institute of Technical Sciences, Serbian Academy of Science and Art, Knez Mihailova St.35, Belgrade, Serbia

Received 15 May 2015; received in revised form 27 May 2015; accepted 29 May 2015
Available online 7 June 2015

Abstract

The impact of the mechanical processing parameters on the alumina grain-size distribution affiliated characteristics and on the γ to α phase transformation rate was investigated. The moderation in the alumina samples behavior has been correlated to the granulometric and mineralogical changes induced by activation via an ultra-centrifugal mill. The assessment of the activation process variables influence on the final quality of the product parameters was conveyed in order to optimize the mechanical treatment of the alumina, which otherwise could be regarded as either energetically or economically unsustainable procedure. The Response Surface Method, Standard Score Analysis and Principal Component Analysis were applied as means of the mechanical activation optimization. The r^2 values obtained by developed models were in range from 0.816 to 0.988. The established mathematical models were able to precisely predict the quality parameters in a broad range of processing parameters. The Standard Score Analysis emphasized that the optimal output sample was obtained using a sieve mesh of 120 μm set of processing parameters (SS=0.96). Diverse comparison analyses disclosed that the optimal set of activation process parameters could reduce the negative effect of γ-alumina samples immanent properties on the final score, and furthermore to enhance the rate of γ to α transition which would improve energetic and economic sustainability of the alumina phase transformation procedure.

Keywords: A. Milling; B. Electron microscopy; B. Grain size; D. Al_2O_3; E. Refractories; E. Thermal applications; Response Surface Analysis

1. Introduction

Alumina (Al_2O_3) is a structurally complex oxide which is characterized by diverse phases, and as such it may exist in its thermodynamically stable state or in one of the meta-stable modifications [1]. Up to the present, researches recognized more than fifteen different crystallographic phases of alumina which can undergo a variety of transitions before reaching the most stable corundum structure (α-Al_2O_3) [2–4]. The alumina polymorph manifestations may vary depending on the processing techniques. Also, the phase transition sequence can take place by various routes. The extensive area of implementation makes the alumina a common ceramic material especially when it is in its stable ultrafine α-Al_2O_3 modification. The conventional procedures for synthesizing of α-Al_2O_3 involve procedures such as precipitation, mechanical milling, vapor-phase reactions, hydrothermal processes, as well as combustion or sol–gel methods [5,6]. Alpha alumina (α-Al_2O_3) is habitually utilized due to its exceptional combination of physicochemical properties such as high melting point, superb wear resistance and good chemical, thermal, and mechanical stability [5–7]. Ultrafine α-Al_2O_3 is a technologically valuable raw material with considerable potential for a wide range of applications including refractory and high strength composites, electronic ceramics and catalysts [8–12].

The thermo-mechanical synthesis is one of the most frequently applied methods in the production of α-Al_2O_3. This procedure requires extensive mechanical milling of the

*Corresponding author. Tel.: +381 11 2650322.
E-mail address: anja.terzic@institutims.rs (A. Terzić).

http://dx.doi.org/10.1016/j.ceramint.2015.05.158
0272-8842/

Nomenclature

MS	sieve mesh size, μm
NRR	number of rotor revolutions, rotations per minute (rpm)
CI	current intensity, A
MAP	mechanical activation period, min
CRS	circumferential rotor speed, m/s
Q	capacity, i.e. batch size of mechanical activator, kg/h
SEC	specific energy consumption (engine power/mill capacity), kW h/t
d_1, d_2	mesh sizes of the sieves, μm[1]
R_1, R_2	accumulated retained masses, %1
d'	average grain size, μm[1]
d_{95}	mesh size appropriate to 95% of accumulated passing mass, μm[1]
n	level of micronization kinetics[1]
S_t	calculated (theoretical) specific surface area, m^2/kg[1]
P	portion of α-Al_2O_3 in the sample, %

γ-Al_2O_3, which is combined with thermal treatment [13]. Thusly obtained micro-sized particles can be of great advantage when they are employed in ceramic composites with advanced performances due to the large surface areas availability and improved grain-size related characteristics [13–15]. The synthesis method includes solid state thermally driven transformations from γ- to α-Al_2O_3. The extent of conversion to the corundum structure depends on the temperature and thermal treatment duration. The atomic motion in the solid state is generally accelerated by destruction of the structure order which is induced by mechanical force, i.e. extensive mechanical milling [16–19]. The γ-Al_2O_3 phase transition coupled with the high activation energy enhances the rate of α-Al_2O_3 nucleating, as a result producing a dense agglomeration-free and homogeneous α-Al_2O_3 with a controlled grain size and decreasing the phase transition temperature [20–22]. Even though numerous methods have been developed with an aim to decrease the α-Al_2O_3 phase transition temperature, i.e. to increase the content of α-Al_2O_3 in the treated material, the mechanical activation was proved as the one of the most effective procedures [13,23,24].

The optimization of the mechanical activation as a part of a synthesis method practically represents a necessity because the ultra-fine grinding can be regarded as unsustainable due to low mill capacity and high energy consumption. The Response Surface Methodology (RSM) was applied in the optimization procedure of the alumina activation as an effective analytical tool [25–27]. The main asset of RSM is minimized number of experimental runs which in return are able to provide sufficient information for statistically valid results. The RSM equations describe effects of the test variables on the monitored responses, determine test variables interrelationships and represent the combined effect of all test variables in the observed responses, enabling the efficient exploration of the process. As the main objective of this study was to assess the quality of the alumina activated via ultra-centrifugal mill Retsch ZM-1 using different process parameters, several product parameters (d_1/d_2, R_1/R_2, d', n, d_{95}, S_t and P) were determined. The influence of NRR, CI, MAP, CRS, and Q on alumina quality parameters was monitored. Experimentally obtained and/or calculated results were subjected to analysis of variance (ANOVA) to show relations between applied assays. In order to enable more inclusive comparison between investigated samples, the Standard Score (SS) was introduced. The Principal Component Analysis (PCA) was applied to classify and discriminate analyzed samples. The goal of this study was to select the optimal set of activation process parameters which could be able to reduce the negative effect of γ-alumina samples immanent properties on the final score by using multiple comparison analyses, and thereby to enhance the rate of γ to α transition which would improve energetic and economic sustainability of the alumina phase transformation procedure.

2. Experimental: materials and methods

2.1. Characterization of the alumina

The investigation was conducted on a sample of commercial high-purity γ-alumina obtained from the manufacturer Alcoa, USA [28]. The original γ-alumina powder was produced by the Bayer process. The chemical analysis performed by a PinAAcle 900 atomic absorption spectrometer (Perkin-Elmer, USA) confirmed that gamma alumina sample was extra pure. The weight loss of the investigated sample was less than 5%. According to the X-ray diffraction analysis conducted on a Philips PW-1710 automated diffractometer using a Cu tube operated at 40 kV and 30 mA, major crystalline phase in the alumina sample was γ-Al_2O_3. The grain size distribution analysis obtained via cyclo-sizer (Warman International LTD, Australia) specified the mean grain diameter value as 7.20 μm. The specific surface area of the starting γ-Al_2O_3 sample was 47.95 m^2/g and the density was 2.4 g/cm^3. The γ-Al_2O_3 grain-size distribution is shown in Fig. 1.

The synthesis of the alpha alumina consisted of two phases: mechanical and thermal treatment. During the first phase the starting γ-Al_2O_3 powder was activated by means of a high speed rotor activator – an ultra centrifugal mill Retsch ZM-1 (Retsch GmbH, Germany) [25,29]. The ultra centrifugal activator was used in the investigation because its ability of rapid size reduction of brittle materials down to the analytical fineness. The motion of the mill's rotor around its fixed ring sieve resulted in the alumina grain size reduction due to

[1]Parameters are derived and/or calculated from grinding kinetic model based on Rosin–Rammler–Sperling (RRS) equation [13,25,29]. The parameters d' and n are obtained by analytical procedure from the diagrams that are described by the equation: $\log\log\frac{100}{R_i} = n\log d_i - n\log d' + \log\log e$, i=1 or 2

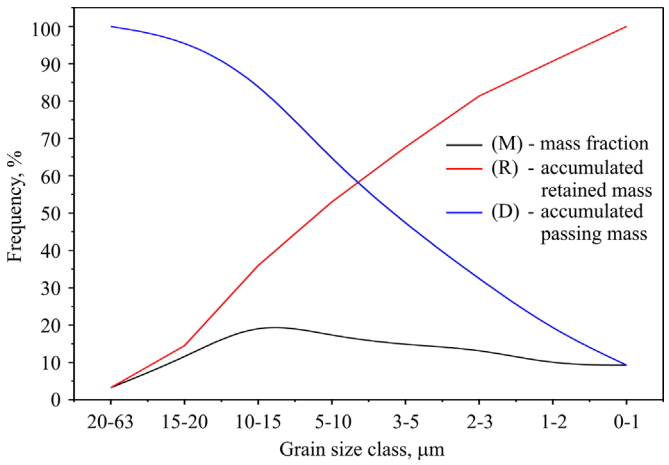

Fig. 1. The grain-size distribution of the initial alumina sample.

incurred impact and shearing effects. The activation procedure was conducted according to the following pattern: the initial alumina sample passed through the hopper with splash-back protection onto the rotor; from that point the centrifugal acceleration threw the treated material outward using huge amount of energy; afterwards the alumina was pre-crushed on the impact with wedge-shaped rotor teeth that moved at a high speed; and finally the processed alumina was being micronized between the rotor and the ring sieve [25,29]. The activator had batch size of 300 ml and stainless steel grinding tools. The applied set of sieves had trapezoid holes of 80, 120, 200 and 500 μm sizes. The established activation periods ranged from 30 to 300 min. The obtained final fineness was generally less than 40 μm depending on the activation environment, i.e. adopted process parameters.

The isothermal treatment of the activated alumina samples in a laboratory furnace (CWF – Chamber Furnace, Carbolite, UK) was the second phase in the synthesis. The material was fired at elevated temperatures ranging from 1000 to 1200 °C, with 50 °C step and delay of 2 h at each temperature of investigation. The applied heating rate was 10 °C/min. The obtained α-Al_2O_3 was compared with the reference α-alumina sample from Alcoa [28].

According to the differential thermal analysis (Shimadzu, DTA-50) the γ-alumina possesses rather amorphous structure at room temperature, but an initial recrystallization in a solid-phase takes place at 250–300 °C involving the growth of γ-Al_2O_3 crystals through the amorphous layers [13,30]. Further phase transformations proceed via various alumina modifications (δ, θ, etc.) and the crystal structures of these modifications resemble that of γ-alumina to high extent [13,31]. The curve of the pure α-Al_2O_3 normally exhibits no significant peaks [13,31].

The portion of α-Al_2O_3 in the alumina samples (at ambient and after treatment at elevated temperatures) was determined via quantitative XRD analysis on a Philips PW-1710 diffractometer. The activated alumina samples, coated with Au films for improvement of the conductivity prior to imaging, were also analyzed by means of a JEOL JSM-5800 scanning electron microscope (JEOL, Japan).

2.2. Statistical analyses

Achieved results of the alumina mechanical activation were expressed by their mean values, for each individual experiment. Assembled data were subjected to ANOVA in order to estimate the effects of process variables. A successful classification and discrimination of the samples gained by different process parameters were conducted by means of the PCA. Pattern recognition technique was applied within results descriptors to characterize and differentiate all observed samples. The evaluation of RSM, ANOVA and PCA analyses of the obtained results was performed using StatSoft Statistica 10.0® software [32]. The following second order polynomial (SOP) model was fitted to the experimental data. Nine models of the following form were developed to relate nine responses (Y) and five process variables (X):

$$Y_k^l = \beta_{k0}^l + \sum_{i=1}^{2} \beta_{ki}^l \cdot X_i + \sum_{i=1}^{2} \beta_{kii}^l \cdot X_i^2 + \beta_{k12}^l \cdot X_1 \cdot X_2,$$
$$k = 1-5, l = 1-\mathrm{p}, \quad (1)$$

where: β_{k0}^l, β_{ki}^l, β_{kii}^l, β_{k12}^l are constant regression coefficients; Y_k^l, either: d_1; d_2; R_1; R_2; d'; n; d_{95}; S_t; and P; while X_1 is NRR; X_2 is CI; X_3 is MAP; X_4 is CRS; and X_5 is Q.

2.3. Determination of normalized standard scores

The SS are evaluated using chemometric approach on the experimentally measured and/or determined d_1, d_2, R_1, R_2, d', n, d_{95}, S_t and P in order to get a more complex observation of the samples ranking. Min–max normalization is one of the most frequently applied techniques for comparison of various characteristics of complex samples determined using multiple measurements, where samples are ranked based on the ratio of raw data and extreme values of the utilized measurement [33]. Since the units and the scale of the data from various physical and chemical characteristics are different, the data in each data set should be transformed into normalized scores, dimensionless quantity derived by subtracting the minimum value from the raw data, and divided by the subtract of maximum and minimum value, according to following equations:

$$\bar{x}_i = 1 - \frac{\max\limits_i x_i - x_i}{\max\limits_i x_i - \min\limits_i x_i, \quad \forall i} \quad (2)$$

in case of "the higher, the better" criteria (used only for MAP score), or

$$\bar{x}_i = \frac{\max\limits_i x_i - x_i}{\max\limits_i x_i - \min\limits_i x_i, \quad \forall i} \quad (3)$$

in case of "the lower, the better" criteria, where x_i represents the raw data.

The sum of normalized scores of a sample for different measurements when averaged gives a single dimensionless value termed as SS. The SS is a specific combination of data from different measuring methods with no unit limitation. This

approach also enables the ease of employing some others set of samples to this elaboration in the future comparisons.

The purpose of this study of alumina mechanical activation was to statistically analyze the characteristic parameters of activation procedure and activation device, and to optimize the procedure regarding energetic and economical sustainability.

3. Results and discussion

An assessment of the benefits of ultra centrifugal mill Retsch ZM-1 application in the γ-alumina activation was conducted in the experiment's initial stage. Prior to this estimation, the comparison and evaluation of the obtained operation parameters (MAP, CRS, Q, SEC) as well as the values of product parameters (mean grain diameter, theoretical specific surface area and portion of α-alumina) were performed. The mesh sizes of initial sieves applied in the experiment were 80, 120, 200 and 500 μm for experimental sequences No I (MS80), No II (MS120), No III (MS200), and No IV (MS500). The number of rotations per minute (NRR) in each experimental sequence were either 10,000 or 20,000. Activation periods varied from 30 min to 300 min. The quality of the activated alumina, as an input for the thermal stage of the synthesis, was studied in terms of d_1, d_2, R_1, R_2, d', n d_{95}, S_t and P. The exact experimental results obtained during conducted alumina activation are given the Table 1. The descriptive statistics data and optimal ranges are presented in Table 2.

The measured and/or determined parameters obtained by statistical analysis can be assigned to two different categories. The first category defines principal characteristics of the activated product (d'; d_{95}, S_t and P). The second category establishes the activation procedure efficiency (MAP and SEC). Theoretically the ideal outcome of the experiment would be when the minimal d′ value, and the maximal S_t and P values are correlated with minimal activation period (MAP) and minimal energy consumption (SEC). However, an interrelation defined in this manner is rarely obtained under experimental conditions. Therefore, the optimal ranges of the parameters have to be established and mutually correlated.

Regarding averaged experimental values presented in Table 2, the shortest activation period (MAP = 87.5 min) was obtained for the experimental sequence MS80. This activation procedure required maximal energy (SEC = 4317.3 kW h/t), however the micronized alumina was characterized by the low mean diameter value (d' = 4.9 μm). Consequently, the obtained S_t (84.3 m^2/g) and P (37.8%) values were high. Experimental sequences MS120 and MS200 produced activated alumina samples with much alike d' values: 5.7 μm and 6.1 μm, respectively. The SEC value for the MS120 sequence was slightly higher by being 1656.6 kW h/t, in comparison with SEC (1600.6 kW h/t) obtained for MS200 sequence. The MAP values applied for treatment in the experimental sequences MS120 and MS200 were 105.0 min and 121.3 min, respectively. The difference between S_t values determined in the scrutinized procedures was insignificant: S_t^{MS120} = 82.4 m^2/g and S_t^{MS200} = 81.5 m^2/g. The obtained α-alumina portion in activated sample was higher for the MS120 sequence. Relatively long activation period of 142.5 min was recorded for the MS500 experimental sequence. The produced mean grain diameter (d' = 9.9 μm) was higher than those achieved in previously explained experimental sequences. Analogously, the specific surface area and the α-alumina portion in the MS500 sample were low and therefore they can be considered as non-satisfactory. The perceived average values of parameters relevant for the sequences MS120 and MS200 were relatively comparable which required further statistical estimation.

A considerable reduction in a number of variables and the detection of structure in the relationship between measured/calculated parameters, various samples and process parameters that give complimentary information were performed in the PCA analysis. All activated alumina samples were generated by means of different processing treatments as it was shown by experimental data given in Table 2 and predicted by PCA score plot illustrated in Fig. 2. The full auto scaled data matrix with various technological treatment parameters is submitted to PCA.

A scatter plot of the samples using the first two principal components (PCs) issued from PCA of the data matrix is obtained for the visualization of the data trends and the efficiency discrimination of the applied descriptors (Fig. 2.). A neat separation of the observed samples, according to used assays can be seen in the PCA biplot. Activated alumina samples produced in the MS80 experimental sequence are located at the left of the PCA graphic, having the greatest S_t and P values. The samples produced in the MS500 experimental sequence are located at the right side and at the bottom of the graphic having the greatest d_2, R_1, R_2, d', and d_{95} values. The samples produced during MS120 and MS200 experimental sequences are located in the center of the PCA graphic transecting the groups of the MS80 and MS500 results. The descriptive statistics data and optimal ranges table (Table 2) previously highlighted the MS80 as the experimental sequence with the highest obtained specific surface area (S_t) and the highest percentage of α-alumina (P) in a sample which is in the agreement with the PCA score plot. However, the experiment and the statistical analysis showed that high values of S_t and P required activation treatment equipped with high specific energy consumption which cannot be considered satisfactory from neither energetic nor economical point of view. The MS500 experimental sequence gave high d' parameters, while obtained S_t and P values were unjustifiably low in comparison to other experimental sequences, which immediately excluded this sequence from further examination.

The quality results highlighted that the first two principal components, accounting for 81.58% of the total variability can be considered sufficient for the data representation. P (which contributed 12.0% of total variance, based on correlations), R_1 (11.3%), d' (13.8%), n (12.7%), d_{95} (14.9%) and S_t (13.6%) were found the most influential for first factor coordinate calculation, while the contribution of d_1 (11.5%), d_2 (11.5%) and R_2 (66.2%) were the most important variables for second factor coordinate calculation.

Table 1
Experimental parameters of activator, activation procedure and activation product.

Exp. seq.	Activator parameters			Activation procedure parameters				Activated product parameters								
	NRR (rpm)	MS (μm)	CI (A)	MAP (min)	CRS (m/s)	Q (kg/h)	SEC (kW h/t)	d_1 (μm)	d_2 (μm)	R_1 (%)	R_2 (%)	d' (μm)	n	d_{95} (μm)	S_t (m^2/g)	P (%)
I	10,000	80	1.50	170	77.50	0.148	5258.50	5.00	40.00	90.25	1.60	5.26	0.49	19.06	81.50	41
			2.70	150	72.00	0.190	4121.40	5.00	40.00	92.80	1.80	6.05	0.57	25.78	80.78	39
			3.50	100	55.15	0.272	3200.00	5.00	40.00	92.90	2.10	6.57	0.58	26.72	79.98	38
			3.90	70	46.35	0.550	2856.32	5.00	40.00	94.25	2.90	7.85	0.63	29.56	77.20	38
	20,000		2.30	75	112.00	0.159	5850.00	5.00	40.00	89.90	5.10	2.05	0.40	13.38	90.50	40
			2.70	60	105.50	0.295	5300.75	5.00	40.00	90.60	7.00	3.25	0.43	15.59	90.05	39
			3.20	45	95.00	0.420	4200.65	5.00	40.00	91.50	8.00	4.01	0.46	16.22	89.00	37
			3.70	30	85.90	0.520	3750.90	5.00	40.00	92.00	9.00	4.52	0.48	18.50	85.00	30
II	10,000	120	1.55	200	77.50	0.165	1958.80	7.00	40.00	95.20	4.00	6.24	0.51	31.71	80.66	41
			1.85	170	70.90	0.310	1697.60	7.00	40.00	96.50	4.50	7.02	0.60	33.64	77.85	39
			2.95	130	52.13	0.580	1541.85	7.00	40.00	97.50	6.00	7.65	0.63	34.44	76.72	38
			3.80	80	45.50	0.720	1269.85	7.00	40.00	97.80	6.50	8.57	0.65	40.11	70.92	38
	20,000		2.50	85	115.90	0.170	2005.40	7.00	45.00	94.00	1.50	2.15	0.41	14.87	90.20	40
			2.75	75	107.26	0.350	1768.49	7.00	45.00	95.70	2.00	3.83	0.45	16.82	90.00	38
			3.30	55	99.20	0.630	1652.00	7.00	45.00	96.00	1.90	4.95	0.48	18.45	88.50	36
			4.20	45	86.50	0.850	1358.99	7.00	45.00	96.50	2.80	5.21	0.50	19.76	84.65	30
III	10,000	200	1.60	250	75.50	0.390	1921.25	8.00	45.00	95.20	2.20	6.60	0.52	32.69	79.78	38
			2.20	200	70.12	0.520	1591.50	8.00	45.00	96.80	3.60	7.15	0.60	35.10	77.80	37
			3.30	150	51.58	0.800	1500.20	8.00	45.00	98.40	5.50	8.02	0.64	39.50	72.20	35
			4.10	100	44.60	0.900	1200.85	8.00	45.00	98.90	6.00	8.96	0.65	42.00	69.90	35
	20,000		2.50	90	118.70	0.450	1995.26	7.00	38.00	94.00	1.90	2.95	0.42	16.90	89.50	37
			2.80	70	105.23	0.620	1700.51	7.00	38.00	95.40	2.00	4.01	0.46	25.90	89.00	37
			3.50	60	97.10	0.870	1600.00	7.00	38.00	96.00	3.00	5.12	0.49	28.90	88.20	35
			4.30	50	86.63	1.100	1295.00	7.00	38.00	97.40	5.00	5.76	0.50	30.20	86.00	29
IV	10,000	500	1.70	300	76.20	0.410	1369.60	10.00	50.00	99.50	4.00	9.96	0.69	50.25	68.47	30
			2.20	240	70.50	0.590	1150.60	10.00	50.00	98.50	5.10	10.05	0.70	56.80	67.10	29
			2.95	180	51.10	0.790	1057.10	10.00	50.00	98.70	6.20	13.29	0.75	60.90	65.20	26
			3.40	120	49.00	1.010	942.20	10.00	50.00	98.75	8.50	15.25	0.85	70.90	63.80	26
	20,000		2.70	90	116.80	0.650	1677.60	9.00	45.00	99.20	4.30	6.98	0.52	36.10	76.30	28
			2.90	80	110.10	0.870	1299.90	9.00	45.00	99.50	5.50	7.14	0.56	43.80	75.90	28
			3.60	70	105.24	0.980	1179.90	9.00	45.00	99.60	7.00	7.98	0.57	45.30	72.50	25
			4.50	60	87.60	1.150	1041.85	9.00	45.00	99.80	8.00	8.79	0.65	48.10	71.10	20

The ANOVA analysis exhibited the significant independent treatment variables as well as interactions of these variables. In this investigation, ANOVA was conducted by StatSoft Statistica, ver. 10 to highlight the significant effects of independent variables to the responses, and to indicate which of responses were significantly affected by the variation of the treatment combinations (Table 3).

It was disclosed that SOP models for all variables were statistically significant. The response surfaces were fitted to these models. The d_1 calculation was affected by a NRR × CRS term in the SOP model, statistically significant at $p < 0.10$ level. The calculation of d_2 was most influenced by the quadratic term of MS. This term was found statistically significant at $p < 00.05$ level, 95% confidence limit. The quadric term of CRS also influenced the d_2 calculation, but at the $p < 00.10$ significance level. The calculation of d' was affected by linear term of MS in SOP model, statistically significant at $p < 00.05$ level. R_1 and R_2 calculations were affected by NRR and CI linear terms ($p < 00.05$ level) as well as by CRS ($p < 00.10$ level). The interchange terms of NRR × MAP and CI × MAP (statistically significant mostly at $p < 00.05$ level) and MAP × CRS (statistically significant mostly at $p < 00.10$ level) made influence on the R_1 and R_2 calculations. The calculations of n are influenced by linear term of CI and the interchange terms of CI × MAP in SOP model, statistically significant at $p < 00.05$ level, as well as the MAP × CRS ($p < 00.10$ level). The evaluation of d_{95} was mostly affected by linear term of MS, and interchange terms of NRR × MAP and MAP × CRS (all statistically significant at $p < 00.05$ level). The impact of linear terms of MS in SOP model was very important for S_t and P calculations.

The established interrelations with either MS parameter solely or MS combined with another process parameter can be anticipated because d_1 and d_2 parameters are derived from the values of the points on the grain-size distribution diagrams of produced activated samples. In addition to that, the R_1 and R_2 are parameters that represent accumulated retained masses which correspond to the d_1 and d_2, and by such they are also reliant on the MS. Additionally, parameters d', d_{95}, and S_t originate from the grinding kinetic model based on Rosin–Rammler–Sperling equation [13,25,29] and, therefore they are directly correlated with the grain size distribution of the

Table 2
Descriptive statistics of activated alumina sample.

	MS	CI	MAP	CRS	Q	SEC	d_1	d_2	R_1	R_2	d'	n	d_{95}	S_t	P
Min.	80	1.5	30.0	46.4	0.1	2856.3	5.0	40.0	89.9	1.6	2.1	0.4	13.4	77.2	30.0
Max.		3.9	170.0	112.0	0.6	5850.0	5.0	40.0	94.3	9.0	7.9	0.6	29.6	90.5	41.0
Ave.		2.9	87.5	81.2	0.3	4317.3	5.0	40.0	91.8	4.7	4.9	0.5	20.6	84.3	37.8
SD		0.8	49.6	23.1	0.2	1066.2	0.0	0.0	1.5	3.0	1.9	0.1	5.9	5.1	3.4
Var.		0.6	2457.1	534.7	0.0	1136830.8	0.0	0.0	2.3	9.0	3.5	0.0	35.4	26.2	11.4
Min. opt.		–	–	–	–	–	–	–	–	–	6.0	0.5	25.0	75.0	33.0
Max. opt.		–	–	–	–	–	–	–	–	–	6.5	0.6	26.0	80.0	35.0
Min.	120	1.6	45.0	45.5	0.2	1269.9	7.0	40.0	94.0	1.5	2.2	0.4	14.9	70.9	30.0
Max.		4.2	200.0	115.9	0.9	2005.4	7.0	45.0	97.8	6.5	8.6	0.7	40.1	90.2	41.0
Ave.		2.9	105.0	81.9	0.5	1656.6	7.0	42.5	96.2	3.7	5.7	0.5	26.2	82.4	37.5
SD		0.9	55.9	25.3	0.3	261.5	0.0	2.7	1.2	1.9	2.1	0.1	9.7	7.1	3.4
Var.		0.8	3128.6	638.7	0.1	68360.4	0.0	7.1	1.5	3.7	4.4	0.0	95.0	49.8	11.4
Min. opt.		–	–	–	–	–	–	–	–	–	7.0	0.5	30.0	70.0	38.0
Max. opt.		–	–	–	–	–	–	–	–	–	7.5	0.6	35.0	75.0	39.0
Min.	200	1.6	50.0	44.6	0.4	1200.9	7.0	38.0	94.0	1.9	3.0	0.4	16.9	69.9	29.0
Max.		4.3	250.0	118.7	1.1	1995.3	8.0	45.0	98.9	6.0	9.0	0.7	42.0	89.5	38.0
Ave.		3.0	121.3	81.2	0.7	1600.6	7.5	41.5	96.5	3.7	6.1	0.5	31.4	81.5	35.4
SD		0.9	72.2	25.7	0.2	275.7	0.5	3.7	1.7	1.7	2.0	0.1	7.9	7.8	2.8
Var.		0.9	5212.5	662.6	0.1	75987.1	0.3	14.0	2.8	2.7	4.1	0.0	63.1	60.4	8.0
Min. opt.		–	–	–	–	–	–	–	–	–	7.5	0.6	35.0	80.0	30.0
Max. opt.		–	–	–	–	–	–	–	–	–	8.0	0.7	45.0	85.0	36.0
Min.	500	1.7	60.0	49.0	0.4	942.2	9.0	45.0	98.5	4.0	7.0	0.5	36.1	63.8	20.0
Max.		4.5	300.0	116.8	1.2	1677.6	10.0	50.0	99.8	8.5	15.3	0.9	70.9	76.3	30.0
Ave.		3.0	142.5	83.3	0.8	1214.8	9.5	47.5	99.2	6.1	9.9	0.7	51.5	70.0	26.5
SD		0.9	88.6	26.1	0.2	232.9	0.5	2.7	0.5	1.7	3.0	0.1	11.0	4.7	3.1
Var.		0.7	7850.0	681.1	0.1	54260.0	0.3	7.1	0.2	2.7	8.7	0.0	120.1	22.0	9.7
Min. opt.		–	–	–	–	–	–	–	–	–	9.0	0.7	50.0	65.0	26.0
Max. opt.		–	–	–	–	–	–	–	–	–	10.0	0.7	60.0	70.0	31.0

activated sample. However, the SOP model also proved that parameters like number of rotations, current intensity, mill capacity and the circumferential rate of the mill engine, including their correlations with MS also determine output data.

The data in the Table 3 also give inquiry in the values of residual variance, where the lack of fit variation represents other contributions except for the higher order terms. A notable lack of fit generally shows that the model failed to represent the data in the experimental domain at points which were not included in the regression [34]. All SOP models had negligible lack of fit tests. Therefore, it can be concluded that all of the models represented the data satisfactorily.

The coefficient of determination (r^2), which is defined as the ratio of the explained variation to the total variation, is described by its magnitude [35,36]. The r^2 is also the proportion of the variability in the response variable, which is obtained by the regression analysis. A high r^2 is suggestive that the variation was accounted and that the data fitted satisfactorily to the proposed model. The r^2 values for d_1 (0.966), d_2 (0.896), R_1 (0.910), R_2 (0.896), d' (0.990), n (0.988), d_{95} (0.988), S_t (0.985) and P (0.988) could be considered as satisfactory. This also means that d_1 and d_2, and consequently R_1 and R_2, were precisely chosen on the grain-size diagram of an activated alumina sample which led to accurate determination of all important activated product parameters using RRS equation [13,25,29]: d', d_{95}, and S_t. The r^2 values showed the excellent fitting of the proposed model to the experimentally obtained results.

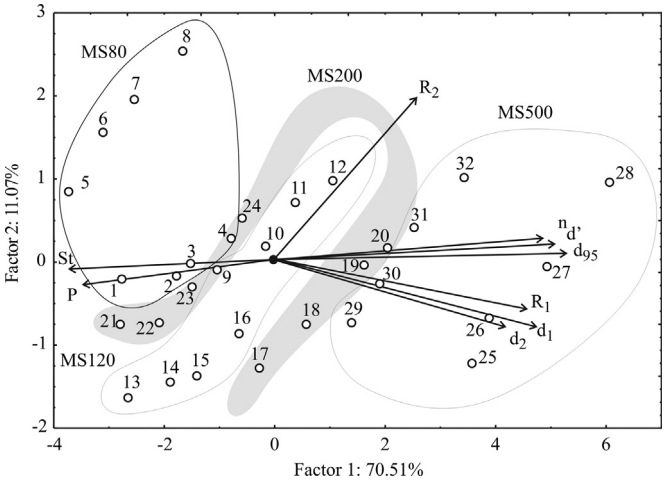

Fig. 2. PCA biplot for characteristics of alumina sample.

The most important response parameters were plotted as three-dimensional diagrams for experiment data visualization, as well as for the purpose of observation of the regression models fitting to the experimental data (Fig. 3.). The 3D graphics were plotted for MS120 as one of the experimental

Table 3
The analysis of variance for parameters of activated alumina sample.

	d_f	d_1	d_2	R_1	R_2	d'	n	d_{95}	S_t	P
NRR	1	0.18	0.25	1.59*	6.94*	0.02	0.0006	26.86**	5.42	1.49
MS	1	0.75	1.30	0.63	0.00	1.84*	0.0008	112.76*	20.09*	9.82*
MS^2	1	0.00	32.42*	0.00	2.43	0.16	0.0008	0.01	4.76	1.38
CI	1	0.13	0.23	3.07*	6.76*	0.00	0.0021*	16.43	4.06	0.04
CI^2	1	0.00	9.70	1.12	4.83	0.01	0.0003	18.01	0.21	0.12
MAP	1	0.03	0.31	0.01	1.78	0.04	0.0003	10.19	1.68	0.99
MAP^2	1	0.66	0.45	2.59	0.14	0.11	0.0003	11.80	0.23	0.65
CRS	1	0.28	1.00	3.38**	5.68**	0.01	0.0009	27.60**	1.96	1.62
CRS^2	1	0.52	18.68**	1.27	1.00	0.01	0.0002	1.31	0.22	2.92
NRR × MS	1	0.10	4.49	2.26	1.51	0.00	0.0004	20.72**	0.05	1.74
NRR × CI	1	0.09	14.71	0.02	2.36	0.00	0.0000	7.38	0.19	0.04
NRR × MAP	1	0.34	0.92	3.64*	7.21*	0.00	0.0007	32.71*	2.37	1.22
NRR × CRS	1	0.89**	8.62	4.29	0.42	0.00	0.0008	14.37	1.76	3.70*
MS × CI	1	0.12	2.36	2.71	1.37	0.07	0.0006	22.12**	0.00	0.78
MS × MAP	1	0.00	2.47	0.10	0.87	0.82	0.0009	3.06	0.00	0.65
MS × CRS	1	0.13	3.14	2.11	1.55	0.03	0.0007	26.71**	0.00	1.41
CI × MAP	1	0.07	3.02	2.57*	6.79*	0.01	0.0018*	22.32**	1.56	0.49
CI × CRS	1	0.01	13.75	0.64	3.91	0.03	0.0002	14.96	0.00	0.00
MAP × CRS	1	0.34	2.07	4.61**	6.39**	0.00	0.0013**	38.00*	1.38	1.18
Error	12	2.93	59.18	24.57	16.53	2.60	0.0041	75.51	31.19	11.59
r^2		0.966	0.869	0.910	0.896	0.990	0.988	0.988	0.985	0.988

*Significant at $p < 00.05$ level.
**Significant at $p < 00.10$ level (95% confidence limit, error terms have been found statistically insignificant).

sequences that gave the most appropriate results based on the conclusions from the conducted statistical analysis.

The SS, as the mean value of standard score transformed from the initial data obtained with different assays (d', n, d_{95}, S_t and P) for every item, was computed by attributing equal weight to the each calculated and/or measured parameter. SS is a dimensionless value which has a consistent correspondence with observed assays. The SS provides a suitably accurate rank of alumina samples even though it is a relative index and may not represent a specific property of an investigated sample. When the SS value is above 0.700, it stands for the high standard regarding alumina samples properties. Application of the standard score analysis and disclosure of the SS of different alumina samples and different processing parameters can be referenced for developing strategies for improving the final product characteristics. The SS analysis of experimental measurements/calculations highlighted optimal processing parameters which are presented in the Table 4.

According to standard score analysis, the optimal sample was obtained using No. 4 (MS500) set of processing parameters because the obtained SS was equal to 1.00. Other set of parameters, No. 1 (MS80) and No. 3 (MS120) gave SS values 0.85 and 0.96, respectively. Both SS values – for the MS80 and MS120 can be considered as satisfactory. However, the MS120 is preferable option due to the higher SS values and two and half times lower specific energy of consumption (SEC) used during the mechanical treatment. The obtained SS value for MS200 set of parameters can be considered as an unacceptable by being only 0.29. If the MS200 set of parameters is excluded from the evaluation due to the result of the standard score analysis, the MS500 and MS120 set of parameters can be regarded as appropriate. However, the MS500 set of parameters cannot be considered as the best option, because the experimental analysis pointed out on inadequate output values such as: too high mean grain diameter, small specific surface area and low α-Al_2O_3 portion in the activated sample. The chosen set of processing parameters (MS, CI, NRR, MAP, and CRS) for is the MS120 sequence gave relatively low SEC, and adequate product parameters (d′, S_t and P), which categorized this treatment as a cost-effective and energetically sustainable. Therefore, the MS120 set of parameters can be regarded as the optimal for the alpha alumina production.

The P value, i.e. the portion of α-phase in the alumina, increased from 10% in the starting γ-alumina sample [13] to the average value of 37.5% for the alumina that was mechanically activated using the MS120 set of parameters. The samples of non-activated alumina (starting γ-alumina) and activated alumina (MS120, MAP = 105 min, $d' = 5.7$ μm and $P = 37.5\%$) were further submitted to the thermal treatment according to the procedure given in the Experimental Chapter. The resulting increase in portion of α-Al_2O_3 phase in the original and activated alumina samples regarding temperature of thermal treatment is presented in Fig. 4.

The applied thermal treatment further induced the α-Al_2O_3 content increase in the activated alumina sample. Namely, from the initial 37.5%, the P reached the value of 95% after thermal treatment at 1200 °C. The alumina sample which contains 95% of alpha phase can be considered as extra pure with properties corresponding to that of commercial Alcoa alpha-alumina sample [13,28]. The non-activated sample contained significantly lower content of α-phase at all temperatures of investigation. The P parameter of non-activated alumina reached its maximum of 86% at the highest

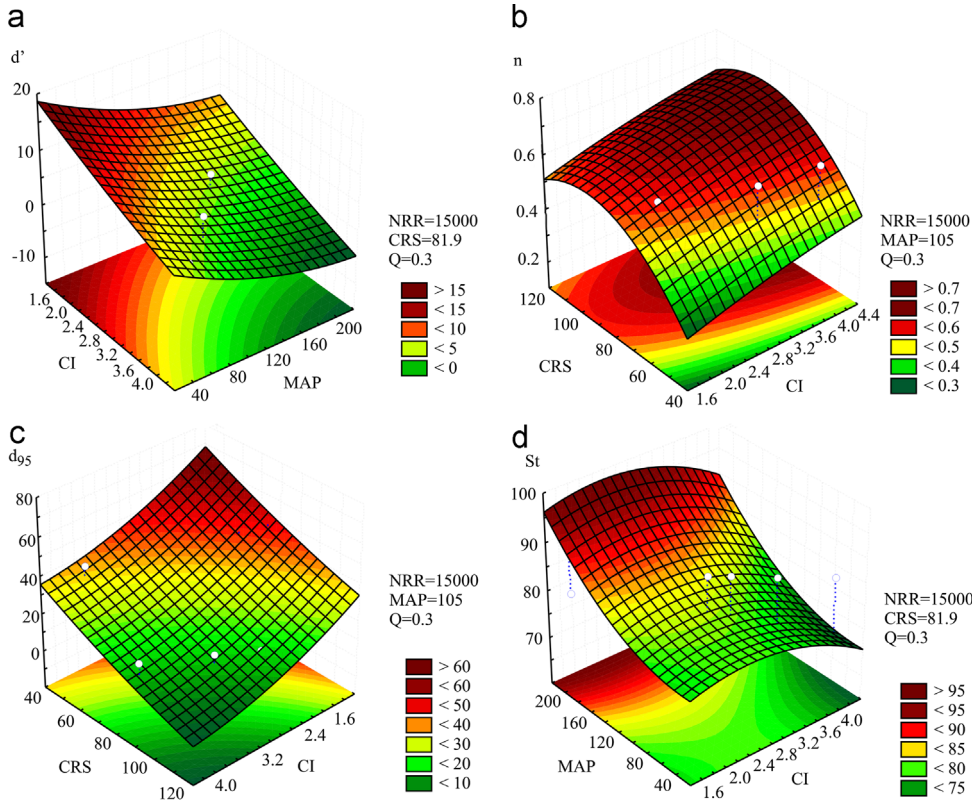

Fig. 3. Visualization of the most important response parameters determined by SOP model.

Table 4
Standard score analysis for alumina processing parameters.

No.	MS	CI	MAP	CRS	Q	SEC	d_1	d_2	R_1	R_2	d'	n	d_{95}	S_t	P	SS
1	80	2.70	150	72.0	0.19	4121.40	5	40	92.8	1.8	6.05	0.57	25.78	80.78	39	0.85
2	120	1.85	170	70.9	0.31	1697.60	7	40	96.5	4.5	7.02	0.60	33.64	77.85	39	0.96
3	200	4.10	100	44.6	0.90	1200.85	8	45	98.9	6.0	8.96	0.65	42.00	69.90	35	0.29
4	500	1.70	300	76.2	0.41	1369.60	10	50	99.5	4.0	9.96	0.69	50.25	68.47	30	1.00

temperature of investigation. Thereby, the mechanical activation conducted according to the MS120 set of parameters contributed to the increase in rate of alpha to gamma phase transition in the alumina sample. Also, thermo-mechanical synthesis produced alumina sample with higher α-Al_2O_3 content than that of a sample produced via thermal treatment solely.

The SEM microphotographs of alumina samples produced via MS80, MS120, MS200 and MS500 activation set of parameters are given in Fig. 5 (a, b, c, and d), respectively.

The microphotograph of alumina activated according to the MS500 set of parameters (Fig. 5d) exhibits large and relatively angular – almost rhombic grains. Alumina samples produced in MS200 and MS120 experimental sequences (presented in Fig. 5c and b, respectively) are characterized by smaller grains that are less angularly and more roundly shaped. The MS80 set

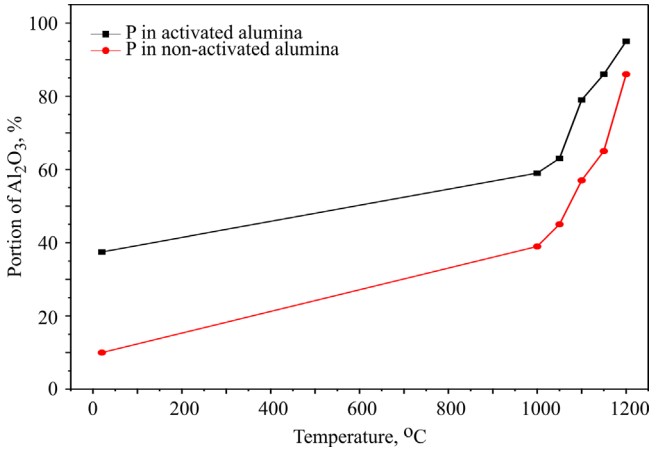

Fig. 4. The α-phase portion in alumina samples regarding treatment temperature.

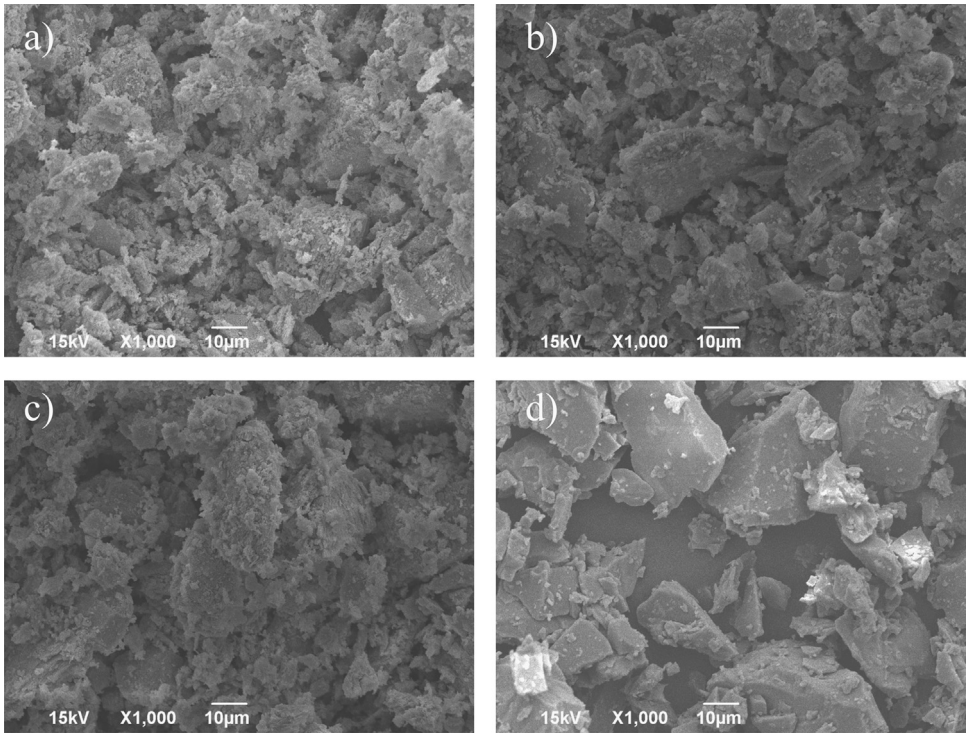

Fig. 5. SEM of activated alumina obtained during experimental sequences: (a) MS80; (b) MS120; (c) MS200; (d) MS500.

of activation parameters produced the alumina sample with high percentage of grains with rather small diameters (Fig. 5a). The agglomeration is a negative side-effect of the mechanical activation and the extent of agglomeration is tightly connected with the crystallite size decrease [37]. Therefore, the transition of alumina through various meta-stable phases might induce agglomeration at some point. Agglomerates usually consist of round particles, i.e. θ-Al_20_3 crystals which are not pseudo-morphs from δ-Al_20_3 rhombs [38,39]. The MS500, MS200 and MS120 samples were generally agglomeration free, however an intensive milling during MS80 sequence produced material with very small grain diameter and certain tenancy to agglomerate.

The SEM analysis revealed a size reduction upon activation of alumina samples that depended on the treatment parameters. Different mean diameters can be seen appropriate to the mesh sizes and processing parameters applied. The smallest grains are registered for the MS80 sequence which is in accordance with the statistical analysis. The biggest mean grain diameter was noticed in the MS500 sequence. The difference in mean grain diameters of MS120 and MS200 sequences was accounted for only 6%, however the Standard Score analysis highlighted the MS200 set of parameters as an unacceptable due to the low SS value. The average grain size of MS120 sequence is only 15% larger than that of MS80 sequence, and having in mind the results and conclusions obtained during optimization, the alumina produced with MS120 set of parameters can be considered as the optimal outcome.

4. Conclusion

The presented investigation was conducted with an aim to optimize the activation treatment via ultra-centrifugal mill as a part of thermo-mechanical synthesis of alumina using statistic methods. The RSM was utilized in the analysis as a method of reduction of experimental runs number that provides sufficient information for statistically valid results. Using PCA and revealing the coordinates of different alumina samples, the position regarding quality data and directions for the improving of their characteristics was realized. A complex influence of linear and nonlinear terms of second order polynomial model was exhibited by ANOVA calculation of the response parameters. The standard score analysis was used in the evaluation of micronized alumina quality, because the quality of a material is influenced by variety of parameters which are altered during treatment.

The statistically suggested processing parameters which would give optimal outcome of the mechanical treatment are: MS = 120 μm, CI = 1.85 A, MAP = 170 min, CRS = 70.9 m/s, SEC = 1697.60 kW h/t and Q = 0.31 kg/h. The quality of thus obtained optimal product is described with following response variables: d_1 = 7 μm, d_2 = 40 μm, R_1 = 96.5%, R_2 = 4.5%, d' = 7.02 μm, n = 0.6, d_{95} = 33.64 μm, S_t = 77.85 m^2/g and P = 39%. Other discussed set of processing parameters showed either high SEC (e.g. MS80) which might be unsustainable from energetic and economical aspect, gave unsatisfactory response values – d', S_t, P (e.g. MS500), or proved unacceptable due to the low SS value (e.g. MS200). Thereby, the

MS120 set of parameters is established as optimal and this parameter combination will be tested in an industrial probe. If the optimized activation procedure proves cost-effective when the procedure is implemented in a fieldwork, it will efficiently contribute to the rationalization and economic and energetic sustainability of the production technology of alumina based advanced and high temperature ceramics.

Acknowledgments

This investigation was supported by Serbian Ministry of Education, Science and Technological Development and it was conducted under following projects: ON 172057, III 45008, TR 31055 and TR 33007.

References

[1] V. Edlmayr, M. Moser, C. Walter, C. Mitterer, Thermal stability of sputtered Al_2O_3 coatings, Surf. Coat. Tech. 204 (2010) 1576–1581.
[2] I. Levin, D. Brandon, Metastable alumina polymorphos: crystal structure and transition sequences, J. Am. Ceram. Soc. 81 (8) (1998) 1995–2012.
[3] S. Arcaro, F.R. Cesconeto, F. Raupp-Pereira, A.P. Novaesde Oliveira, Synthesis and characterization of LZS/α-Al_2O_3 glass–ceramic composites for applications in the LTCC technology, Ceram. Int. 40 (2014) 5269–5274.
[4] S. Ito, N. Umehara, H. Takata, T. Fujii, Phase transition of γ-Al_2O_3 under hot isostatic pressure, Solid State Ion. 172 (2004) 403–406.
[5] H. Wang, Z. He, D. Li, R. Lei, J. Chen, S. Xu, Low temperature sintering and microwave dielectric properties of $CaSiO_3$–Al_2O_3 ceramics for LTCC applications, Ceram. Int. l40 (2014) 3895–3902.
[6] J.G. Li, X. Sun, Synthesis and sintering behavior of a nanocrystaline α-alumina powder, Acta Mater. 48 (2000) 3103–3112.
[7] B. Zhu, Y. Zhu, X. Lin, F. Zhao, Effect of ceramic bonding phases on the thermo-mechanical properties of Al_2O_3–C refractories, Ceram. Int. 39 (2013) 6069–6076.
[8] S. Dutta, P. Das, A. Das, S. Mukhopadhyayn, Significant improvement of refractoriness of Al_2O_3–C castables containing calcium aluminate nano-coatings on graphite, Ceram. Int. 40 (2014) 4407–4414.
[9] R.K. Pati, J.C. Ray, P. Pramanik, A novel chemical route for the synthesis of nanocrystalline α-Al_2O_3, Mater. Lett. 44 (7) (2000) 299–303.
[10] P. Palmero, F. Kern, M. Lombardi, R. Gadow, Role of immiscible and miscible second phases on the sintering kinetics and microstructural development of nano-crystalline a-Al_2O_3-based materials, Ceram. Int. 37 (2011) 3547–3556.
[11] Z. Wang, H. Mao, S.K. Saxena, The melting of corundum (Al_2O_3) under high pressure conditions, J. Alloy. Compd. 299 (2000) 287–291.
[12] M. Razavi, A. Rajabi-Zamani, M. Rahimipour, R. Kaboli, M. Shabani, R. Yazdani-Rad, Synthesis of Fe–TiC–Al_2O_3 hybrid nanocomposite via carbothermal reduction enhanced by mechanical activation, Ceram. Int. 37 (2011) 443–449.
[13] A. Terzić, L.j. Andrić, V. Mitić, Assessment of intensive grinding effects on alumina as refractory compound: acceleration of γ to α phase transformation mechanism, Ceram. Int. 40 (2014) 14851–14863.
[14] S. Cava, S.M. Tebcherani, I.A. Souza, S.A. Pianaro, C.A. Paskocimas, E. Longo, J.A. Varela, Structural characterization of phase transition of Al_2O_3 nanopowders obtained by polymeric precursor method, Mater. Chem. Phys. 103 (2007) 394–399.
[15] S. Cava, S.M. Tebcherani, S.A. Pianaro, C.A. Paskocimas, E. Longo, J.A. Varela, Structural and spectroscopic analysis of γ-Al_2O_3 to α-Al_2O_3–$CoA_{l2}O_4$ phase transition, Mater. Chem. Phys. 97 (2006) 102–108.
[16] E. Yalamac, S. Akkurt, Additive and intensive grinding effects on the synthesis of cordierite, Ceram. Int. 32 (2006) 825–832.
[17] S. Barseghyana, Y. Sakka, Mechanochemical activation of aluminum powder and synthesis of alumina based ceramic composites, Ceram. Int. 39 (2013) 8141–8146.
[18] P. Balaz, in: Extractive Metallurgy of Activated Minerals, Elsevier, Amsterdam, 2000, p. 278.
[19] T. Tkacova, in: Mechanical Activation of Minerals, Elsevier, Amsterdam, 1989, p. 293.
[20] K. Okada, A. Hattori, Y. Kameshima, A. Yasumori, Concentration effect of Csq additive on the γ-Al_2O_3 to α-Al_2O_3 phase transition, Mater. Lett. 42 (2000) 175–178.
[21] S. Ghanizadehn, X. Bao, B. Vaidhyanathan, J. Binner, Synthesis of nano α-alumina powders using hydro thermal and precipitation routes: a comparative study, Ceram. Int. 40 (2014) 1311–1319.
[22] F. Dynys, J. Halloran, Alpha alumina formation in alum-derived gamma alumina, J. Am. Ceram. Soc. 65 (9) (1982) 442–448.
[23] J. Li, Y. Pan, C. Xiang, Q. Ge, J. Guo, Low temperature synthesis of ultrafine α-Al_2O_3 powder by a simple aqueous sol–gel process, Ceram. Int. 32 (2006) 587–591.
[24] H. Schaper, L. van Reijen, A quantitative investigation of the phase transformation of gamma to alpha alumina with high temperature DTA, Thermochim. Acta 77 (1984) 383–393.
[25] A. Terzić, L. Pezo, L.j. Andrić, Chemometric analysis of the influence of mechanical activation on the mica quality parameters, Ceram. Int. 41 (2015) 8894–8903.
[26] M. Arsenović, S. Stanković, L. Pezo, Z. Radojević, Prediction and fuzzy synthetic optimization of process parameters in heavy clay brick production, Ceram. Int. 39 (2013) 2013–2022.
[27] U. Ulusoy, Application of ANOVA to image analysis results of talc particles produced by different milling, Powder Technol. 188 (2008) 133–138.
[28] ⟨https://www.alcoa.com/global/en/home.asp⟩.
[29] L.j. Andrić, A. Terzić, Z. Aćimović-Pavlović, M. Petrov, Comparative kinetic study of mechanical activation process of mica and talc for industrial application, Compos. Part B Eng. 59 (2014) 181–190.
[30] J. McCallum, T. Simpson, I. Mitchell, Time resolved reflectivity measurements of the amorphous-to-gamma and gamma-to-alpha phase transitions in ion-implanted A120, Nucl. Instrum. Methods B 91 (1994) 60–62.
[31] F. Yen, J. Long Chang, P. Ching Yu, Relationships between DTA and DIL characteristics of nanosized alumina powders during γ to α phase transformation, J. Cryst. Growth 246 (2002) 90–98.
[32] Statistica (Data Analysis Software System), v. 10., Stat-Soft, Inc., USA, (⟨www.statsoft.com⟩), 2010.
[33] T. Brlek, L. Pezo, N. Voća, T. Krička, Đ. Vukmirović, R. Čolović, M. Bodroža-Solarov, Chemometric approach for assessing the quality of olive cake pellets, Fuel Process.Technol. 116 (2013) 250–256.
[34] P. Madamba, The response surface methodology: an application to optimize dehydration operations of selected agricultural crops, LWT-Food Sci. Technol. 35 (2002) 584–592.
[35] NIST/SEMATECH e-Handbook of Statistical Methods, ⟨http://www.itl.nist.gov/div898/handbook/pri/section1/pri11.htm⟩ (2013).
[36] NIST/SEMATECH e-Handbook of Statistical Methods, ⟨http://www.itl.nist.gov/div898/handbook/pri/section3/pri333.htm⟩ (2013).
[37] R. Yang, P. Yu, C. Chen, F. Yen, Phase metastability of nanosized α-Al_2O_3 crystallites, J. Eur. Ceram. Soc. 32 (2012) 2153–2162.
[38] P. Souza Santos, H. Souza Santos, S.P. Toledo, Standard transition aluminas. electron microscopy studies, J. Mater. Res. 3 (2000) 104–114.
[39] A. Boumaza, L. Favaro, J. Ledion, G. Sattonnay, J. Brubach, P. Berthet, A. Huntz, P. Roy, R. Tetot, Transition alumina phases induced by heat treatment of boehmite: an X-ray diffraction and infrared spectroscopy study, J. Solid State Chem. 182 (5) (2009) 1171–1176.